

Spin Glass to Weak Ferromagnetic Transformation in a New Layered Cobaltite: Consequence of Topotactic Reactions with Water at Room Temperature

T. Motohashi,* B. Raveau, V. Caignaert, V. Pralong, M. Hervieu, D. Pelloquin, and A. Maignan

Laboratoire CRISMAT, UMR CNRS ENSICAEN 6508, 6 bd Maréchal Juin, 14050 Caen, Cedex 4, France

Received June 21, 2005. Revised Manuscript Received September 23, 2005

A new $n = 2$ -member of the Ruddlesden–Popper (RP) cobaltite series, $\text{Sr}_{3-\delta}\text{Co}_{1.9}\text{Nb}_{0.1}\text{O}_{6.65-\delta}$, has been stabilized by niobium doping. This oxide reacts topotactically with atmospheric water through hydrolysis/hydration and reduction of cobalt, leading to an oxyhydroxide hydrate derivative, $\text{Sr}_{3-\delta}\text{Co}_{1.9}\text{Nb}_{0.1}\text{O}_{4.86-\delta}(\text{OH})_{3.04}\cdot 0.4\text{H}_2\text{O}$. The reaction with water at room temperature induces a magnetic transformation from a spin glass behavior with a freezing temperature $T_g \approx 50$ K for the pristine RP oxide to weak ferromagnetism with an apparent Curie temperature $T_C \approx 200$ K for the oxyhydroxide hydrate derivative. The spectacular effect of water upon the magnetic properties of this layered oxide is explained by the partial reduction of Co^{4+} into Co^{3+} species, concomitantly inducing a coordination change for cobalt cations that form antiferromagnetic coupling between high-spin Co^{3+} . A generalization of this phenomenon to other layered cobaltites and even iron oxides is considered.

Introduction

The recent discovery of superconductivity in a layered cobaltite, $\text{Na}_{0.3}\text{CoO}_2\cdot y\text{H}_2\text{O}$,¹ has stimulated great attention upon cobalt oxides and their hydrated derivatives. One of the most noticeable features in this superconductor is that superconductivity is induced by intercalation of water molecules. It has been revealed that the superconductive properties of this material is very sensitive to the water content (y) (i.e., superconductivity appears only for $y \cong 1.3$), and the anhydrous $\text{Na}_{0.3}\text{CoO}_2$ and “less”-hydrated $\text{Na}_{0.3}\text{CoO}_2\cdot 0.6\text{H}_2\text{O}$ phases are non-superconductive down to the lowest temperature.^{2,3} The appearance of superconductivity in $\text{Na}_{0.3}\text{CoO}_2\cdot y\text{H}_2\text{O}$ seems to be related to the variety and complexity of the electronic states in cobaltites. It has been widely known that the crystal-field splitting of the Co $3d$ state and the Hund’s coupling energy are comparable in cobaltites such that various kinds of electronic/magnetic phases with different spin states are in a subtle balance, giving us an expectation to induce electronic/magnetic phase transformation triggered by stimulation—such as a hydration reaction.

Studies of the layered Ruddlesden–Popper (RP) cobaltites, $\text{Sr}_{n+1}\text{Co}_n\text{O}_{3n+1-\delta}$,⁴ and more recently of their oxyhydroxide

hydrates⁵ and derivatives involving also the possibility to substitute partially cobalt by titanium⁶ suggest that water reaction may have a particular influence upon the magnetic properties of these oxides, leading for instance to cluster and spin glass behavior. Nevertheless, in the latter case neither the oxidation state of cobalt nor the magnetic properties were investigated for the “as-prepared” anhydrous phase, making difficult the interpretation of their evolution in the course of the hydration reaction. We have thus explored possibilities of stabilization of such RP cobaltites by substituting various transition-metal elements. We report herein on a new oxygen-deficient $n = 2$ -RP member, $\text{Sr}_{3-\delta}\text{Co}_{1.9}\text{Nb}_{0.1}\text{O}_{6.65-\delta}$, and its oxyhydroxide hydrate derivative, $\text{Sr}_{3-\delta}\text{Co}_{1.9}\text{Nb}_{0.1}\text{O}_{4.86-\delta}(\text{OH})_{3.04}\cdot 0.4\text{H}_2\text{O}$. We show that the magnetic property evolves from a spin glass behavior with a freezing temperature $T_g = 50$ K for the anhydrous pristine oxide to weak ferromagnetism with $T_C = 200$ K for the derivative phase. This magnetic transformation, which takes place at room temperature, is explained by a topotactic reaction with water, involving hydration, hydrolysis, and partial reduction of Co^{4+} into Co^{3+} .

Experimental Procedures

The pristine sample was prepared by a conventional solid-state reaction. A powder mixture of SrCO_3 , Co_3O_4 , and Nb_2O_5 with an appropriate ratio of $\text{Sr}_3\text{Co}_{1.9}\text{Nb}_{0.1}\text{O}_{7-\delta}$ was calcined in flowing O_2 gas at 800°C for 12 h. This calcined powder was ground, pelletized, and fired in flowing O_2 gas at 1200°C for 12 h, followed by slow cooling to room temperature. For experimental procedures of the pristine “fresh” sample, the closest attention was paid to prevent

* Corresponding author permanent address: Materials and Structures Laboratory, Tokyo Institute of Technology, 4259 Nagatsuta, Midori-ku, Yokohama 226-8503, Japan. E-mail: t-mot@msl.titech.ac.jp. Phone: +81-45-924-5318. Fax: +81-45-924-5339.

- (1) Takada, K.; Sakurai, H.; Takayama-Muromachi, E.; Izumi, F.; Dilanian, R. A.; Sasaki, T. *Nature (London)* **2003**, *422*, 53.
- (2) Foo, M. L.; Schaak, R. E.; Miller, V. L.; Klimczuk, T.; Rogado, N. S.; Wang, Y.; Lau, G. C.; Craley, C.; Zandbergen, H. W.; Ong, N. P.; Cava, N. P. *Solid State Commun.* **2003**, *127*, 33.
- (3) Karppinen, M.; Asako, I.; Motohashi, T.; Yamauchi, H. *Chem. Mater.* **2004**, *16*, 1693.
- (4) Dann, S. E.; Weller, T. M. *J. Solid State Chem.* **1995**, *115*, 499.

(5) Pelloquin, D.; Barrier, N.; Maignan, A.; Caignaert, V. *Solid State Sci.* **2005**, *7*, 853.

(6) Pelloquin, D.; Barrier, D.; Flahaut, D.; Caignaert, V.; Maignan, A. *Chem. Mater.* **2005**, *17*, 773.

an undesirable hydration reaction. The sintered pellets were put in a vacuum chamber immediately after taking them out of an atmosphere-controlled furnace. The sample was then stored in a glovebox in which water concentration was kept less than 0.05 ppm, and all the sample preparations were carried out in the glovebox. On the other hand, a part of the pristine sample was exposed to air for 7 days to obtain a fully hydrated sample.

X-ray powder diffraction (XRPD) analysis was performed using a Philips X-pert Pro diffractometer (Cu $K\alpha$ radiation) equipped with an atmosphere-controlled chamber (Anton Paar TTK 450), which allows us to measure diffraction patterns at temperatures up to 400 °C. The data were collected in an angular range of $4^\circ \leq 2\theta \leq 120^\circ$ with a standard setup (in open air) and with the chamber and were analyzed with a Rietveld program, FULLPROF.⁷ The sample for electron microscopy study was prepared from the pristine material and directly stocked in the glovebox under argon flow. The crystallites were gently crushed, using CCl_4 as suspension liquid, to avoid as far as possible any trace of water. The flakes were deposited on a holey carbon film, supported by a copper grid. The grid was put on the sample holder in the glovebox and carried up to the JEOL 200CX microscope under argon atmosphere. The intensity of electron beam used in the course of the electron diffraction (ED) investigation was lowered at maximum due to the sensitivity of the sample. Thermogravimetric analysis (TGA) was made with a SETARAM setup in flowing nitrogen gas. The oxygen content, $7-\delta$, was determined by the iodometric titration in flowing argon gas with an accuracy of ± 0.02 . Details in the titration technique are given elsewhere.⁸

Magnetic properties were investigated using a PPMS facility (Quantum Design). Magnetization measurements were carried out with the DC extraction method in a temperature range of $5 \text{ K} \leq T \leq 300 \text{ K}$ and in magnetic fields up to 5 T. AC susceptibility was also measured in an ac-field of 3 Oe with frequencies of 10^2 , 10^3 , and 10^4 Hz.

Results and Discussion

Pristine Sample $Sr_{3-\delta}Co_{1.9}Nb_{0.1}O_{7-\delta}$: Crystal Chemistry and Composition. Starting from the nominal composition of $Sr_3Co_{1.9}Nb_{0.1}O_{7-\delta}$, the pristine pellets prepared with the above experimental condition were well-sintered and bluish black in color, indicating electronic delocalization. However, no transport measurements could be made since the samples reacted with atmospheric water very quickly and collapsed into a fine dark brown powder by exposure to air at room temperature. In contrast, the samples could be kept in the glovebox for several weeks without any alteration of their properties. The XRPD and ED investigations, as well as chemical analyses, were carried out on pristine “fresh” samples in the absence of air (i.e., in argon flow or in a vacuum). Nevertheless, short time of exposure to air of the order of several minutes could not be avoided for electron microscopy and XRPD analyses in order to install the samples in the facility.

The oxygen content of this phase was determined with accuracy by iodometric titration: $O_{6.65}$ per formula. This result leads to an intermediate valency of cobalt between +3 and +4 (i.e., $V_{Co} = +3.57$), bearing in mind that niobium is pentavalent in the structure. However, the EDS analysis

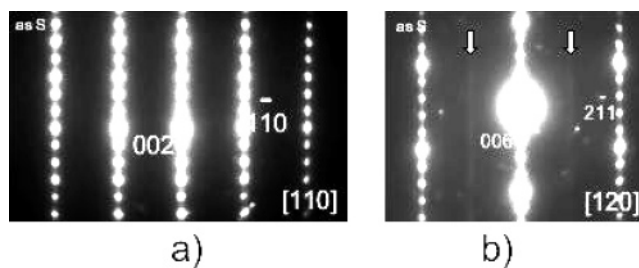
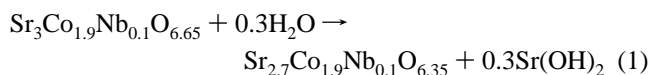


Figure 1. (a) [110] and (b) [120] ED patterns of the pristine oxide of $Sr_{3-\delta}Co_{1.9}Nb_{0.1}O_{6.65-\delta}$. Streaky lines parallel to the c^* axis are indicated with vertical arrows in the latter figure.

performed on more than 50 crystals shows a significant strontium deficiency with respect to the nominal formula implying the cationic composition “ $Sr_{2.7}Co_{1.9}Nb_{0.1}$ ”. Several hypotheses can be put forward to explain this strontium deficiency. Two of them seem more likely. The first one deals with the fact that a part of SrO would not react with cobalt and niobium oxides, such that $Sr_{2.7}Co_{1.9}Nb_{0.1}O_{6.35}$ would be formed directly at high temperatures, with secondary amorphous phases such as SrO , $SrCO_3$ or most probably $Sr(OH)_2$, which is undetectable by XRPD. Nevertheless, starting from the nominal composition of $Sr_{2.7}Co_{1.9}Nb_{0.1}O_{7-\delta}$ does not allow pure and well-sintered samples to be obtained. The second hypothesis would be based on a secondary reaction occurring at the surface of particles examined by EDS analysis: the particles were indeed very small ($\approx 1 \mu\text{m}$ in diameter) and might be highly Sr-deficient in the vicinity of their surface over a thickness of $\approx 200 \text{ \AA}$, resulting in the global composition of $Sr_{2.7}Co_{1.9}Nb_{0.1}O_{6.35}$ according to the reaction:



In the second hypothesis, such an EDS result would not reflect the actual composition of the pristine phase, since the mobility of Sr^{2+} cations and H_2O molecules is not sufficiently high enough to diffuse homogeneously and reach this global composition throughout the sample pellet. Thus, it is not possible to determine the exact value of Sr content in the pristine sample, and we will keep the formula $Sr_{3-\delta}Co_{1.9}Nb_{0.1}O_{6.65-\delta}$ in the following.

An ED study on this phase allowed the reciprocal space to be reconstructed by tilting around the crystallographic axes for the “as-synthesized” pristine sample, which was handled as afore described. The ED patterns evidence a pseudo-tetragonal phase, with $a \approx a_p \approx 3.8 \text{ \AA}$ and $c \approx 20 \text{ \AA}$, where a_p denotes a perovskite subcell. The intense reflections were found to obey the $hkl: h+k+l = 2n$ limiting conditions; both set of cell parameters and I -type symmetry are consistent with the $n = 2$ member of the RP series. The [110] and [120] ED patterns are shown as examples in Figure 1, panels a and b, respectively. However, diffuse streaky lines parallel to the c^* direction are visible, as indicated with vertical arrows in the latter image. They correspond to the appearance of a superstructure with $a_p\sqrt{2} \times a_p\sqrt{2}$, but it is poorly coherent along the c axis. Similar phenomena are rather commonly observed in the RP phases, as a result of

(7) Rodríguez-Cavajal, J.; Anne, M.; Pannetier, J. *FULLPROF Version May 2003*; Laboratoire Léon Brillouin: Saclay, France, 2003.

(8) Maignan, A.; Hebert, S.; Caignaert, V.; Pralong, V.; Pelloquin, D. *J. Solid State Chem.* **2005**, *178*, 868–873.

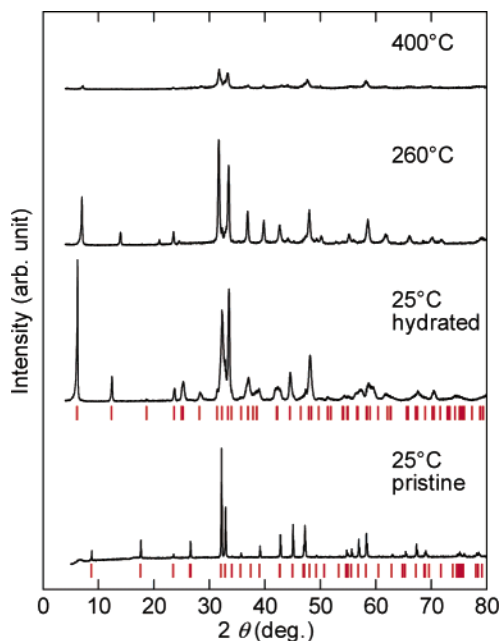


Figure 2. X-ray powder diffraction patterns of the pristine RP oxide, $\text{Sr}_{3-\delta}\text{Co}_{1.9}\text{Nb}_{0.1}\text{O}_{6.65-\delta}$, and its oxyhydroxide hydrate derivative, $\text{Sr}_{3-\delta}\text{Co}_{1.9}\text{Nb}_{0.1}\text{O}_{4.86-\delta}(\text{OH})_{3.04}\cdot 0.4\text{H}_2\text{O}$. Both patterns are indexed in the $I4/mmm$ space group with $a = 3.8483 \text{ \AA}$, $c = 20.108 \text{ \AA}$ for the pristine sample, and $a = 3.786 \text{ \AA}$, $c = 28.42 \text{ \AA}$ for the hydrated sample. The red bars in this figure indicate predicted peak position based on the $I4/mmm$ space group for both the pristine and fully hydrated phases. High-temperature XRD patterns at 260 and 400 °C are also shown.

Table 1. Atomic Coordinates of the Pristine RP Oxide, $\text{Sr}_{3-\delta}\text{Co}_{1.9}\text{Nb}_{0.1}\text{O}_{6.65-\delta}$

atom	Wyck.	x	y	z
Sr1	2b	1/2	1/2	0
Sr2	4e	1/2	1/2	0.1827(3)
Co/Nb	4e	0	0	0.0997(5)
O1	2a	0	0	0
O2	4e	0	0	0.207(2)
O3	8g	0	1/2	0.087(2)

^a Space group: $I4/mmm$ (No. 139), $a = 3.8483(2) \text{ \AA}$, $c = 20.108(1) \text{ \AA}$, $\chi^2 = 3.6$, $R_1 = 12.5\%$.

superstructure and lowered symmetry.⁹ The ED investigation excluded the existence of other RP members or intergrowth defects as a possible explanation for the Sr-deficiency (i.e., the analyzed cation ratio of $\text{Sr}_{2.7}\text{Co}_{1.9}\text{Nb}_{0.1}$). This result supports the fact that the Sr-deficiency does not originate from high-temperature phase formation but from room temperature hydrolysis, resulting in the formation of amorphous $\text{Sr}(\text{OH})_2$.

The XRPD pattern of this phase (Figure 2) can be indexed in a tetragonal cell, space group $I4/mmm$ with the refined cell parameters: $a = 3.8483(2) \text{ \AA}$ and $c = 20.108(1) \text{ \AA}$. These values are in good agreement with those obtained by the ED analyses. A refinement of the crystal structure by the Rietveld method leads to atomic coordinates as listed in Table 1, characteristic of the $n = 2$ member of the RP cobaltite series,⁴ with a statistical distribution of cobalt and niobium in the structure. These results confirm the classical structure model of the RP series (Figure 3a) but do not allow us to obtain an accurate occupation probability of the Sr and

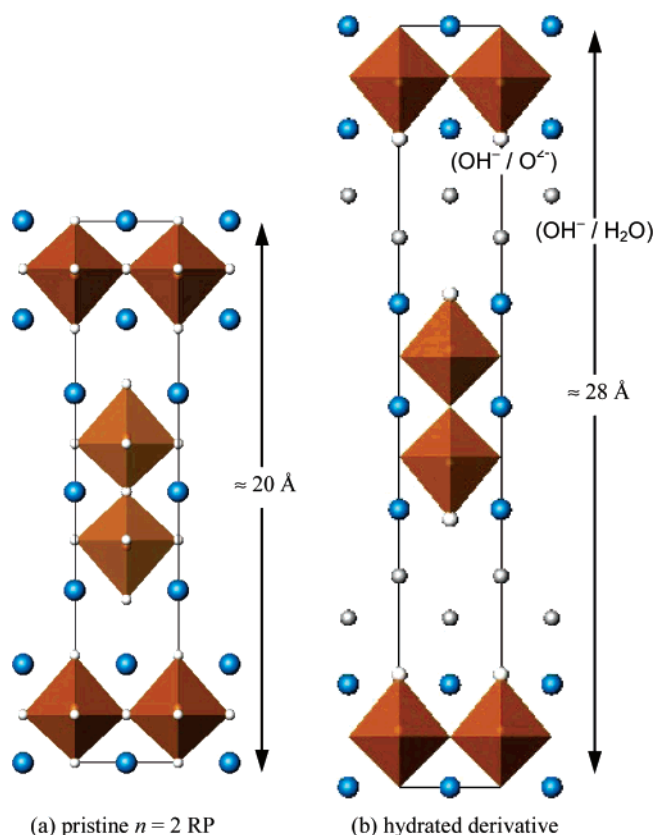


Figure 3. Schematic illustration of the structural models of (a) the pristine RP oxide, $\text{Sr}_{3-\delta}\text{Co}_{1.9}\text{Nb}_{0.1}\text{O}_{6.65-\delta}$, and (b) its oxyhydroxide hydrate derivative, $\text{Sr}_{3-\delta}\text{Co}_{1.9}\text{Nb}_{0.1}\text{O}_{4.86-\delta}(\text{OH})_{3.04}\cdot 0.4\text{H}_2\text{O}$.

O sites since the reliability factor remains high ($R_{\text{Bragg}} = 12\%$) due to strong preferred orientation in the sample and fluorescence phenomena from cobalt atoms.

Topotactic Reactions with Water: Oxyhydroxide Hydrate Derivative $\text{Sr}_{3-\delta}\text{Co}_{1.9}\text{Nb}_{0.1}\text{O}_{4.86-\delta}(\text{OH})_{3.04}\cdot 0.4\text{H}_2\text{O}$. By prolonged exposure to air, the XRD pattern of the pristine sample changes rapidly by reacting with atmospheric water. In Figure 4, two strong peaks at $2\theta \approx 32.2^\circ$ and 32.9° characteristic of the 105 and 110 reflections, respectively, in the RP oxide $\text{Sr}_{3-\delta}\text{Co}_{1.9}\text{Nb}_{0.1}\text{O}_{6.65-\delta}$ have almost disappeared and at the same time new peaks have appeared around 6.2° and 33.5° , within only 2 h. The latter set of reflections being indexed $d_{002} \approx 14.2 \text{ \AA}$ and $d_{112} \approx 2.66 \text{ \AA}$ in the hydrated phase. After exposure to air for 7 days, an essentially single-phased compound was obtained whose XRD pattern (Figure 2) was successfully indexed in a tetragonal cell, space group $I4/mmm$ with $a = 3.786(1) \text{ \AA}$ and $c = 28.42(1) \text{ \AA}$. Note that one observes a decrease in the a -axis length as previously observed in a similar compound.⁵ The diffraction peaks of this hydrated phase are significantly broadened, indicating a deterioration of the crystallinity of the compound. Moreover, one observes a very anisotropic profile of the XRPD pattern, indicating the presence of strains and delamination of the lamellae. Thus, a refinement of the structure was unsuccessful for these data. Nevertheless, this phase is isotopic to the titanocobaltite $\text{Sr}_3\text{Co}_{1.7}\text{Ti}_{0.3}\text{O}_5(\text{OH})_2\cdot x\text{H}_2\text{O}$ whose structure has previously been established.⁶ Thus a structural model (Figure 3b) can be proposed, where hydroxyl groups and H_2O molecules

(9) Maignan, A.; Martin, C.; Van Tendeloo, G.; Hervieu, M.; Raveau, B. *J. Mater. Chem.* **1998**, *8*, 2411.

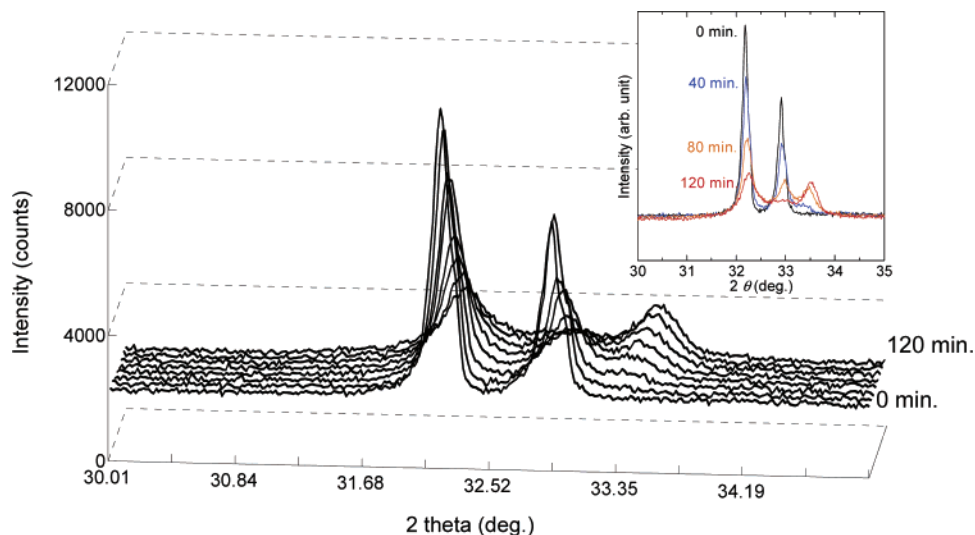


Figure 4. Evolution of the XRD pattern ($30^\circ \leq 2\theta \leq 35^\circ$) recorded for the pristine sample with respect to air-exposure time. The pristine RP oxide has almost been transformed into its oxyhydroxide hydrate derivative only within 2 h in open air.

form double layers[OH, H₂O] inserted between two [Sr(O,-OH)] layers, according to the formula Sr_{3- δ} Co_{1.9}Nb_{0.1}X_{9- δ} with X = O, OH, and H₂O.

For ED investigations of this derivative phase, 10 crystallites of the pristine Sr_{3- δ} Co_{1.9}Nb_{0.1}O_{6.65- δ} phase were selected. They were then exposed to air for 2 h, kept mounted on the sample holder, re-introduced in the microscope, and re-characterized. The EDS analyses revealed no variation of the cationic composition after air exposure. However, phase transformations were found to take place. It clearly appears that the final state is not reached after 2 h in air, and instead some intermediate states can be observed depending on the crystallites. This feature is illustrated by three typical [100] ED patterns shown in Figure 5. In the first one (Figure 5a), the majority phase is of the $n = 2$ -RP member, but the existence of weak and diffuse extra reflections indicates a secondary phase being stabilized in the crystallite with $a \approx a_p \approx 3.8 \text{ \AA}$, $c \approx 12.5 \text{ \AA}$, and a P -type space group (marked with white arrows in the enlarged image). In the second ED pattern (Figure 5b), the majority phase is now the P -type phase, whereas there remain only weak spots associated with the pristine $n = 2$ -RP phase (see the enlarged image). Note that the sharpness of the spots is diminished with regard to those of the pristine phase. Last, in the third pattern (Figure 5c), a set of nodes appears that corresponds to the final derivative phase with $a \approx a_p \approx 3.8 \text{ \AA}$, $c \approx 28 \text{ \AA}$. The ED pattern of the fully hydrated sample exposed to air for 7 days is identical to the latter. The lack of stability of this oxyhydroxide hydrate, which transforms rapidly into the RP structure under the electron beam, does not allow a complete reconstruction of the reciprocal space. Taking into account only the intense spots of the latter phase, the conditions of reflection suggest an I -type space group for the final phase, but a deteriorated crystallinity of the grains forbids a determination of the real symmetry. One indeed observes weak diffuse lines along the reciprocal c^* axis, indicating that the periodicity is not perfect along this direction. Moreover, it clearly appears that the latter phase is poorly crystallized since most of the crystallites exhibit ED patterns

characteristic of mica-like compounds, involving rotating and tilting phenomena of the stacked lamellae [see weak intensity of the $0kl$ ($k \neq 2n$) spots]. Since the crystallites have not been mechanically handled between the first (the pristine RP oxide) and second (its hydrated derivative) ED observations, it is probable that such a morphology results from the hydration mechanism of the present phase and its instability under high vacuum.

At this point, to determine the chemical composition of the hydrated derivative, chemical and thermogravimetric analyses were carried out. The iodometric titration of this derivative phase reveals a significant decrease in the cobalt valency (V_{Co}) with respect to the pristine one, from +3.57 to +3.28. The thermogravimetric analysis for the hydrated sample, carried out in nitrogen flow (Figure 6) shows a large weight loss occurring below about 400°C. It is difficult to divide the thermogravimetric curve into individual steps, as the curve is smooth and complex. Nevertheless, the first step that takes place below 150 °C is rather clear and attributed to the departure of ~ 0.4 mol of “free water”, leading to an oxyhydroxide form whose crystal structure is intermediate between that of the pristine (Figure 3a) and hydrated phases (Figure 3b). This hypothesis is confirmed by a high-temperature XRPD study carried out at 260 °C (Figure 2): the c -axis length is drastically shortened, and a new derivative phase has appeared. On the other hand, the weight loss between 150 and 400 °C, corresponding to 1.52 H₂O per formula, can be attributed to the destruction of OH groups in the structure, involving 3.04 OH per formula. Bearing in mind that the cobalt valence deduced from the chemical titration is +3.28, the formulation of the derivative phase should be Sr_{3- δ} Co_{1.9}Nb_{0.1}O_{4.86- δ} (OH)_{3.04}·0.4H₂O, in agreement with the proposed structural model (Figure 3b) where the “O, OH, H₂O” sites of the medium layers are half-occupied.

A close structural relationship between the pristine and its derivative phases strongly suggests that the reaction of the present $n = 2$ RP cobaltite with water is topotactic. Thus, from the similarity to the action of water upon the iron oxide

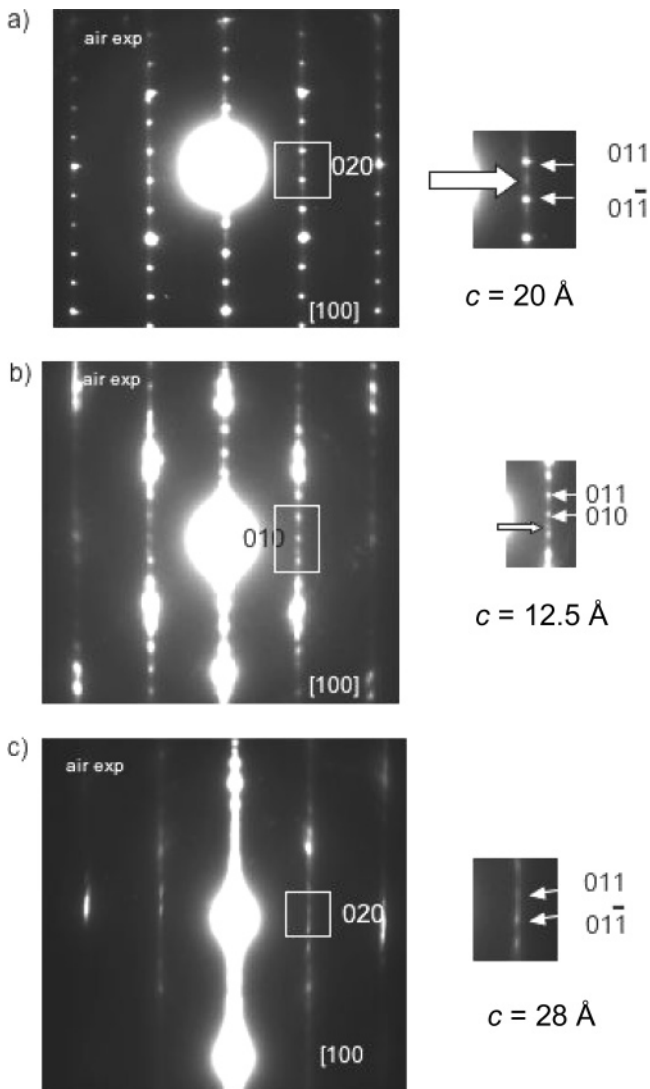
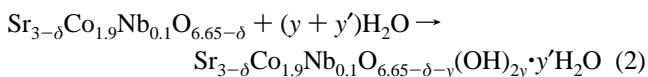


Figure 5. Typical [100] ED patterns observed after 2 h exposure in air, illustrating the structural transformation. (a) The pristine phase with the $n = 2$ -RP structure. A weak spot from a secondary phase is indicated with a right arrow in the enlarged image. (b) The intermediate P -type phase with $c = 12.5$ Å. Diffraction spots from the pristine phase (indicated with a right arrow) are now very weak. (c) The majority I -type phase with $c \approx 28$ Å.

$\text{Sr}_3\text{NdFe}_3\text{O}_{9-\delta}$,¹⁰ a topotactic hydrolysis/hydration can take place according to the equation:



Nevertheless, this equation is not sufficient to describe the formation mechanism of the oxyhydroxide hydrate derivative, since it does not account for the change in the cobalt valency through the reaction with water. Thus, another reaction must also be considered to explain the fact that the cobalt valency has been accordingly reduced from +3.57 to +3.28. The latter corresponds to the reduction of tetravalent cobalt into trivalent cobalt by the action of H_2O at room temperature, observed in several layered cobaltites, as for instance for CoO_2 :¹¹



The topotactic reaction of $\text{Sr}_{3-\delta}\text{Co}_{1.9}\text{Nb}_{0.1}\text{O}_{6.65-\delta}$ with water

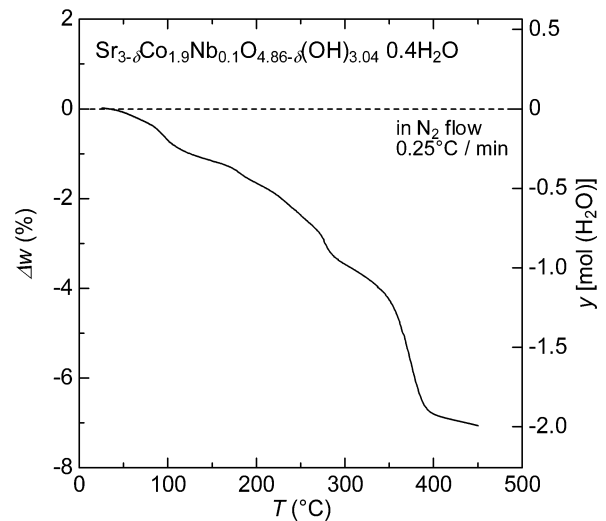
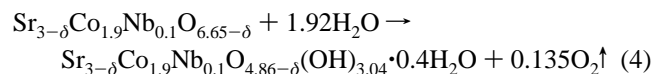


Figure 6. Thermogravimetric curve for the hydrated sample, $\text{Sr}_{3-\delta}\text{Co}_{1.9}\text{Nb}_{0.1}\text{O}_{4.86-\delta}(\text{OH})_{3.04} \cdot 0.4\text{H}_2\text{O}$, recorded in nitrogen flow. The water content (y) was estimated from the sample weight loss, assuming that all of water molecules are completely released from the lattice at 400 °C.

is in fact a combination of these two sorts of reactions that involves hydrolysis, hydration, and reduction of cobalt. The global reaction can be written as:



Magnetic Properties of the Pristine and Oxyhydroxide Hydrate Phases. Considering a significant difference in the structure and cobalt valency between the pristine RP oxide $\text{Sr}_{3-\delta}\text{Co}_{1.9}\text{Nb}_{0.1}\text{O}_{6.65-\delta}$ and the oxyhydroxide hydrate phase $\text{Sr}_{3-\delta}\text{Co}_{1.9}\text{Nb}_{0.1}\text{O}_{4.86-\delta}(\text{OH})_{3.04} \cdot 0.4\text{H}_2\text{O}$, one can anticipate a magnetic modification in the course of the topotactic reaction with water. The temperature dependence of dc magnetization (M) for the pristine RP phase, registered in a magnetic field of 0.3 T (Figure 7a), suggests a typical spin-glass behavior with a freezing temperature T_g of 50 K. This statement is supported by a large hysteresis in the $M(H)$ loop at 5 K (Figure 7b). In the pristine RP phase, the system is subject to magnetic frustration due to strong competing (i.e., ferromagnetic and antiferromagnetic) interactions and disordering phenomena originating from the statistical distribution of Nb at the Co site and the presence of oxygen vacancies.

Surprisingly, the hydrated sample is found to show a totally different behavior compared to the pristine sample: a “Brillouin-like” temperature dependence of magnetization is seen (Figure 7a), clearly indicating that weak ferromagnetism appears after reacting with water. In fact, the $M(H)$ loop of this hydrated derivative shows magnetization increasing abruptly in low fields with a lack of saturation in high fields. The maximum magnetization value of $0.1 \mu_B/\text{Co}$ site in 5 T, being much smaller than the value of the pristine oxide, suggests that the latter is antiferromagnetic. A small spin canting in low magnetic fields would create a ferromagnetic

(10) Pelloquin, D.; Hadermann, J.; Giot, M.; Caignaert, V.; Michel, C.; Hervieu, M.; Raveau, B. *Chem. Mater.* **2004**, *16*, 1715.

(11) Amatucci, G. G.; Tarascon, J. M.; Klein, L. C. *J. Electrochem. Soc.*, **1996**, *143*, 1114.

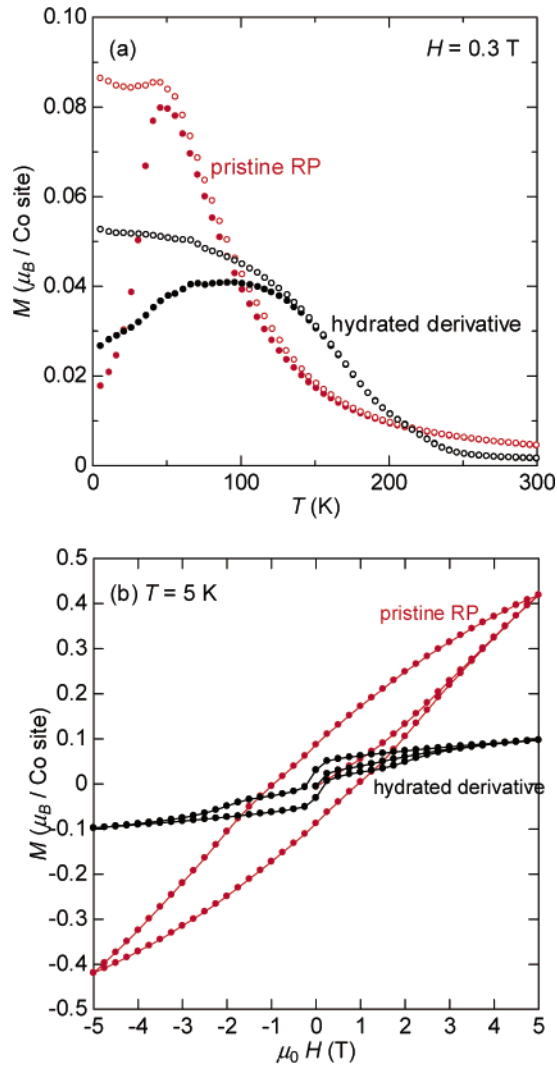


Figure 7. (a) Temperature dependence of dc magnetization (M) for the pristine RP oxide, $\text{Sr}_{3-\delta}\text{Co}_{1.9}\text{Nb}_{0.1}\text{O}_{6.65-\delta}$, and its oxyhydroxide hydrate derivative, $\text{Sr}_{3-\delta}\text{Co}_{1.9}\text{Nb}_{0.1}\text{O}_{4.86-\delta}(\text{OH})_{3.04}\cdot 0.4\text{H}_2\text{O}$. The data were recorded in a magnetic field of 0.3 T. (b) The M vs H loops at 5 K for the pristine RP oxide and its oxyhydroxide hydrate derivative.

like component. Such a very different behavior in low fields is best highlighted by the results of ac susceptibility as shown in Figure 8. The $\chi'(T)$ and $\chi''(T)$ curves of the pristine RP phase clearly depend on frequency and a peak temperature systematically increases with increasing frequency (see inset of the lower panel in Figure 8). The frequency shift, defined as $\Delta T_m/[T_m \Delta(\log f)]$, is determined at 0.04, which is comparable to the values reported for typical spin glass materials.¹² For the hydrated derivative, on the other hand, the peak position (≈ 180 K) in the $\chi'(T)$ curve does not depend on frequency, being in contrast to the pristine RP phase. A Curie-like temperature (T_C) is determined at 200 K from the onset of $\chi''(T)$ that corresponds to the appearance of dissipation linked to weak ferromagnetism.^{13,14} This result indicates that spin canting develops from ≈ 200 K. It is worthy to point out that this transition temperature is much

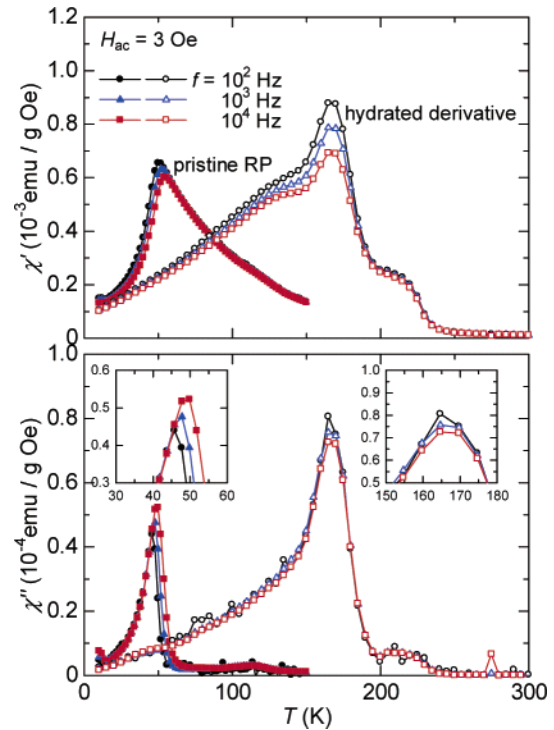


Figure 8. Temperature dependence of ac-susceptibility, χ' (upper panel) and χ'' (lower panel), for the pristine RP oxide, $\text{Sr}_{3-\delta}\text{Co}_{1.9}\text{Nb}_{0.1}\text{O}_{6.65-\delta}$, and its oxyhydroxide hydrate derivative, $\text{Sr}_{3-\delta}\text{Co}_{1.9}\text{Nb}_{0.1}\text{O}_{4.86-\delta}(\text{OH})_{3.04}\cdot 0.4\text{H}_2\text{O}$. The data were recorded in an ac-field of 3 Oe with frequencies of 10^2 , 10^3 , and 10^4 Hz. Closed and open symbols denote the data plots for the pristine RP and its oxyhydroxide hydrate derivative phases, respectively. The magnified plots near the $\chi''(T)$ peaks are shown in the insets of the lower panel.

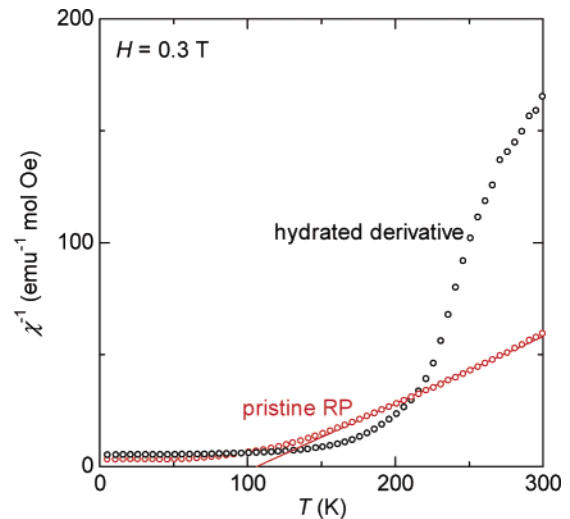


Figure 9. Curie-Weiss plots for the pristine RP oxide, $\text{Sr}_{3-\delta}\text{Co}_{1.9}\text{Nb}_{0.1}\text{O}_{6.65-\delta}$, and its oxyhydroxide hydrate derivative, $\text{Sr}_{3-\delta}\text{Co}_{1.9}\text{Nb}_{0.1}\text{O}_{4.86-\delta}(\text{OH})_{3.04}\cdot 0.4\text{H}_2\text{O}$.

higher than $T_C = 150$ K of the ferromagnetic perovskite cobaltite, $\text{SrCo}_{1-x}\text{Nb}_x\text{O}_{3-\delta}$.^{15,16} Thus, the magnetic behavior of the hydrated sample cannot be explained by a trace of such perovskite impurities.

The Curie-Weiss plots (Figure 9) show very distinct $\chi^{-1}(T)$ curves for the pristine RP phase and its hydrate

(12) Mydosh, J. A. *Spin Glasses: An Experimental Introduction*; Taylor and Francis: London and Washington, DC, 1993.

(13) Mukherjee, S.; Ranganathan, R.; Anilkumar, P. S.; Joy, P. A. *Phys. Rev. B* **1996**, *54*, 9267.

(14) Maignan, A.; Martin, C.; Damay, F.; Raveau, B.; Hejtmanek, J. *Phys. Rev. B* **1998**, *58*, 2758.

(15) Motohashi, T.; Caignaert, V.; Pralong, V.; Hervieu, M.; Maignan, A.; Raveau, B. *Appl. Phys. Lett.* **2005**, *86*, 192504.

(16) Motohashi, T.; Caignaert, V.; Pralong, V.; Hervieu, M.; Maignan, A.; Raveau, B. *Phys. Rev. B* **2005**, *71*, 214424.

derivative. The μ_{eff} value calculated for the former ($3.75 \mu_{\text{B}}$ /Co) could be explained by considering high-spin Co^{3+} and low-spin Co^{4+} , leading to an expected value $\mu_{\text{eff}} = 3.47 \mu_{\text{B}}$.¹⁷ Nevertheless, the presence of large amounts of oxygen vacancy creates different kinds of oxygen coordination for cobalt, which makes very hazardous any interpretations for the spin state of cobalt. In this respect, the topotactic reaction with water most probably creates CoO_5OH polyhedra in which the Co–OH distance is larger than the Co–O ones. This means that the majority Co^{3+} cations may be considered as 5-fold coordinated rather than 6-fold. This tends to stabilize the high-spin state Co^{3+} as in the $\text{Sr}_2\text{CoO}_3\text{Cl}$ oxychloride,¹⁸ which is an antiferromagnet with $T_{\text{N}} = 330$ K.¹⁹ As a consequence, the present hydrate derivative phase is probably a 2D antiferromagnet or a 2D canted weak ferromagnet with high-spin Co^{3+} . The presence of Co^{4+} may disturb the complete antiferromagnetic alignment setting at the origin of spin canting. The change in the $\chi(T)$ curve (Figure 8) could reflect the antiferromagnetic state induced by the reaction with water.

Concluding Remarks

In the present study, we have shown that a layered cobaltite with the $n = 2$ -RP structure, $\text{Sr}_{3-\delta}\text{Co}_{1.9}\text{Nb}_{0.1}\text{O}_{6.65-\delta}$, is immediately transformed into an oxyhydroxide hydrate

derivative, $\text{Sr}_{3-\delta}\text{Co}_{1.9}\text{Nb}_{0.1}\text{O}_{4.86-\delta}(\text{OH})_{3.04} \cdot 0.4\text{H}_2\text{O}$, by reacting with atmospheric water at room temperature. The topotactic reaction with water not only changes the crystal structure and intercalates OH groups and H_2O molecules by hydrolysis–hydration but also concomitantly involves a partial reduction of Co^{4+} into Co^{3+} . As a consequence, a large number of OH groups is located on the anionic sites, in contrast with other cobalt oxyhydroxides reported in previous literature.^{5,6} More importantly, we have demonstrated that the magnetic properties of the material dramatically change from a spin-glass behavior with a freezing temperature $T_{\text{g}} \approx 50$ K to weak ferromagnetism with Curie temperature $T_{\text{C}} \approx 200$ K in the course of the topotactic reaction. Such a possibility opens the door to the exploration of other members of the RP series, not only with cobalt but also with other transition metal elements such as iron. This great ability of water to induce a topotactic reduction of cobalt in layered cobaltites, in a simultaneous action with hydrolysis and hydration, should also be taken into consideration to understand the superconductive properties of “ $\text{Na}_x\text{CoO}_2 \cdot y\text{H}_2\text{O}$ ”, which may as well form $\text{Na}_x\text{CoO}_{2-z}(\text{OH})_z \cdot y\text{H}_2\text{O}$ or $\text{Na}_x(\text{H}_3\text{O}^+)_z\text{CoO}_2 \cdot y\text{H}_2\text{O}$ ^{3,20} with closely related structures.

CM051334W

(17) For the hydrated derivative phase, neither the effective moment (μ_{eff}) nor the Weiss temperature (Θ) can be accurately obtained from the Curie–Weiss plot (Figure 9), as a paramagnetic linear regime does not reach even at 300 K. It is important to recall that above 300 K the sample starts to lose water molecules such that the paramagnetic regime cannot be studied in detail.

- (18) Hu, Z.; Wu, H.; Haverkort, M. W.; Hsieh, H. H.; Lin, H.-J.; Lorenz, T.; Baier, J.; Reichl, A.; Bonn, I.; Felser, C.; Tanaka, A.; Chen, C. T.; Tjeng, L. H. *Phys. Rev. Lett.* **2004**, *92*, 207402.
- (19) Knee, C. S.; Price, D. J.; Lees, M. R.; Weller, M. T. *Phys. Rev. B* **2003**, *68*, 174407.
- (20) Takada, K.; Fukuda, K.; Osada, M.; Nakai, I.; Izumi, F.; Dilanian, R. A.; Kato, K.; Takata, M.; Sakurai, H.; Takayama-Muromachi, E.; Sasaki, T. *J. Mater. Chem.* **2004**, *69*, 2767.